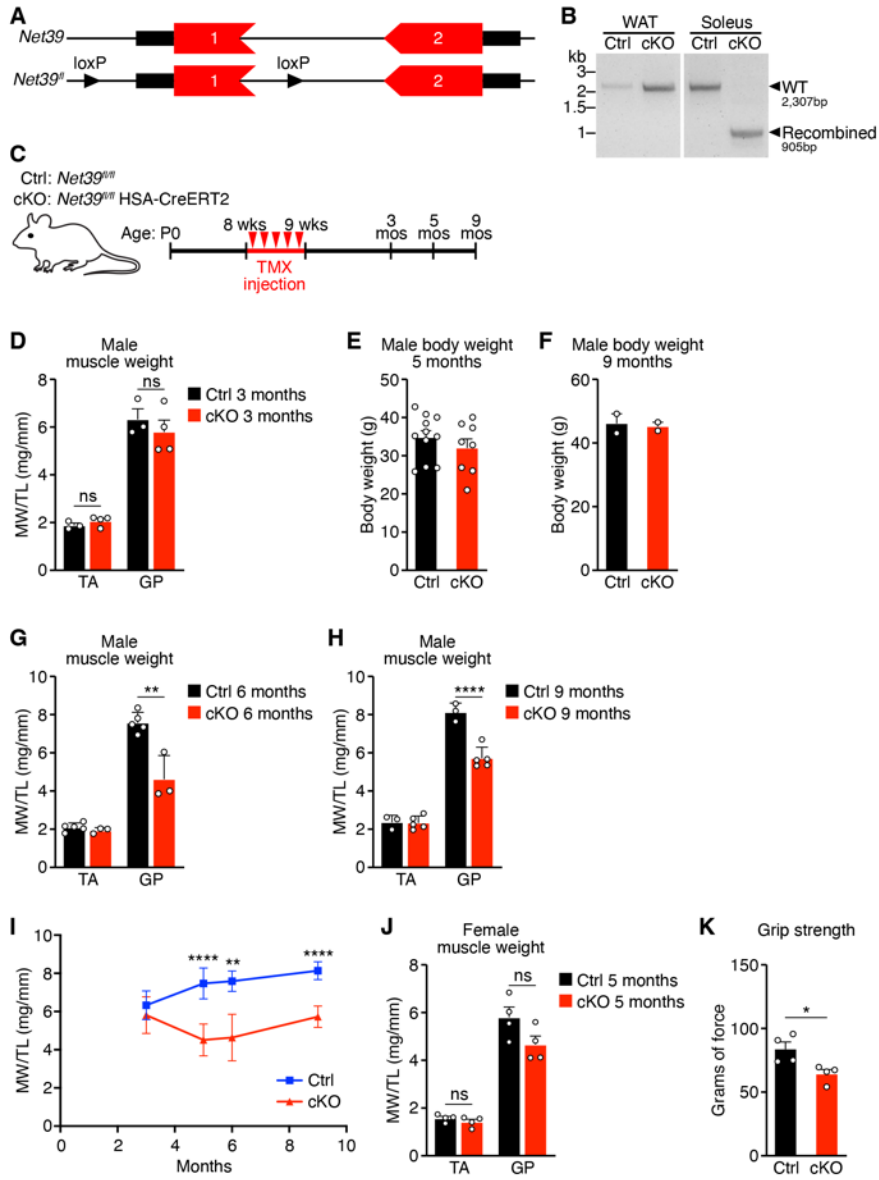


Supplemental Figures

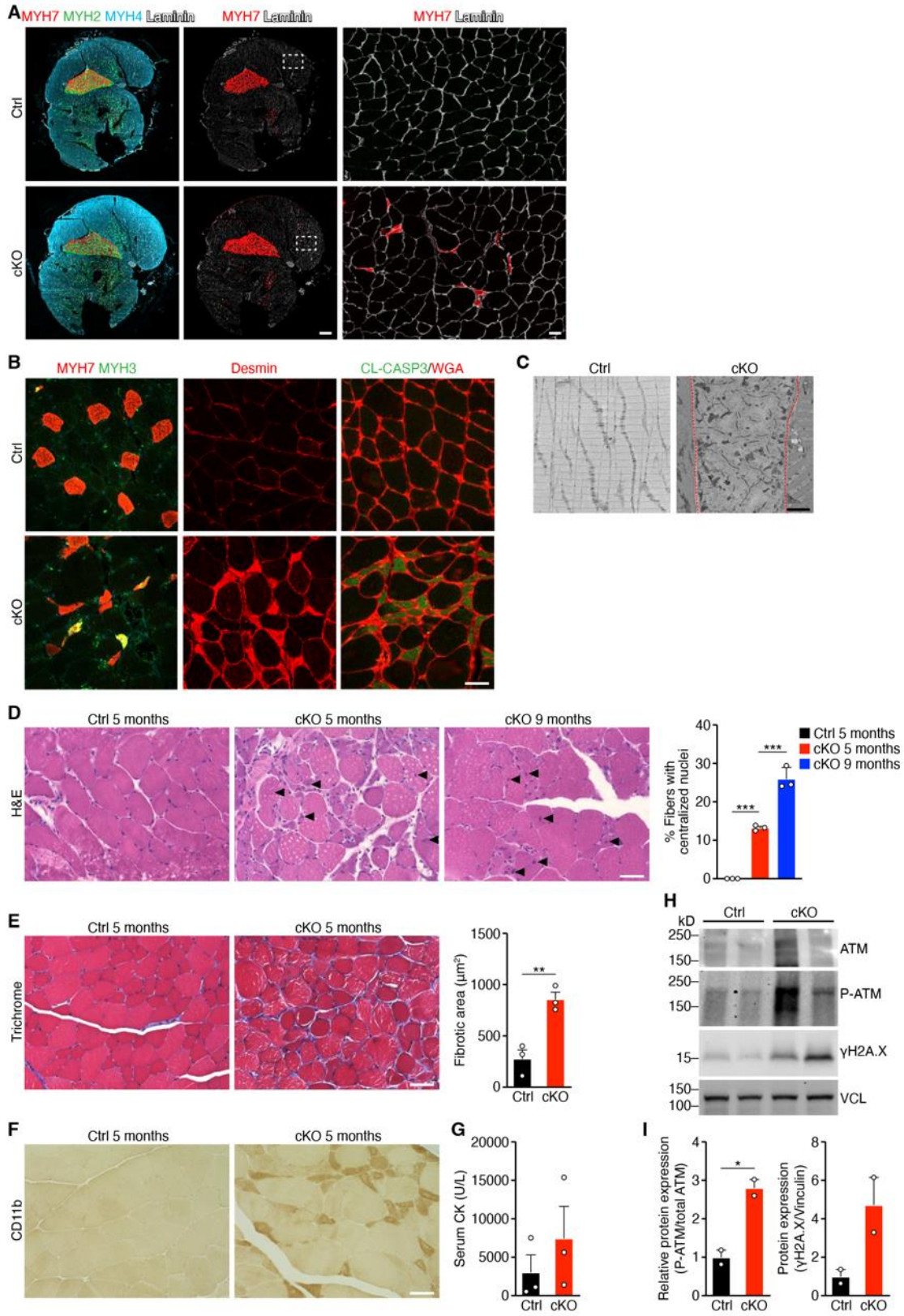


Supplemental Figure 1

Supplemental Figure 1 – Adult deletion of Net39 in adult skeletal muscle leads to muscle wasting without changes in body weight.

- a) Gene structure of the conditional allele for *Net39* (*Net39^{fl}*). Black arrowheads indicate the locations of the loxP sequences inserted. Boxes represent exons. Black boxes denote untranslated regions and red boxes denote the open reading frame.
- b) PCR analysis of recombination at the *Net39* locus in Ctrl and cKO soleus and WAT. Wildtype (WT) allele is 2,307 bp and the recombined allele is 905 bp. WAT: White adipose tissue.
- c) Experimental design for deletion of *Net39* in adult skeletal muscle and analysis of these mice at 3 months, 5 months, and 9 months of age.
- d) Quantification of muscle weight to tibia length ratios for Ctrl and cKO male mice at 3 months of age. TA: tibialis anterior, GP: gastrocnemius-plantaris. ns: Not significant. Statistical comparisons between groups were evaluated by unpaired, two-tailed Student's t-test. N=3-4 mice per group. Data represent mean \pm SEM.
- e) Quantification of body weight for Ctrl and cKO male mice at 5 months of age. N=8-11 mice per group. Data represent mean \pm SEM.
- f) Quantification of body weight for Ctrl and cKO male mice at 9 months of age. N=2 mice per group. Data represent mean \pm SEM.
- g) Quantification of muscle weight to tibia length ratios for Ctrl and cKO male mice at 6 months of age. TA: tibialis anterior, GP: gastrocnemius-plantaris. ** $p < 0.01$. Statistical comparisons between groups were evaluated by unpaired, two-tailed Student's t-test. N=3-5 mice per group. Data represent mean \pm SEM.

- h) Quantification of muscle weight to tibia length ratios for Ctrl and cKO male mice at 9 months of age. TA: tibialis anterior, GP: gastrocnemius-plantaris. **** $p < 0.0001$. Statistical comparisons between groups were evaluated by unpaired, two-tailed Student's t-test. N=3-5 mice per group. Data represent mean \pm SEM.
- i) Time-course of muscle weight to tibia length ratios for Ctrl and cKO male GP muscle. ** $p < 0.01$, **** $p < 0.0001$. Statistical comparisons between groups were evaluated by unpaired, two-tailed Student's t-test.
- j) Quantification of muscle weight to tibia length ratios for Ctrl and cKO female mice at 5 months of age. TA: tibialis anterior, GP: gastrocnemius-plantaris. ns: Not significant. Statistical comparisons between groups were evaluated by unpaired, two-tailed Student's t-test. N=4 mice per group. Data represent mean \pm SEM.
- k) Grip strength measurements of Ctrl and cKO male mice at 5 months of age. * $p < 0.05$. Statistical comparisons between groups were evaluated by unpaired, two-tailed Student's t-test. N=4 mice per group. Data represent mean \pm SEM.

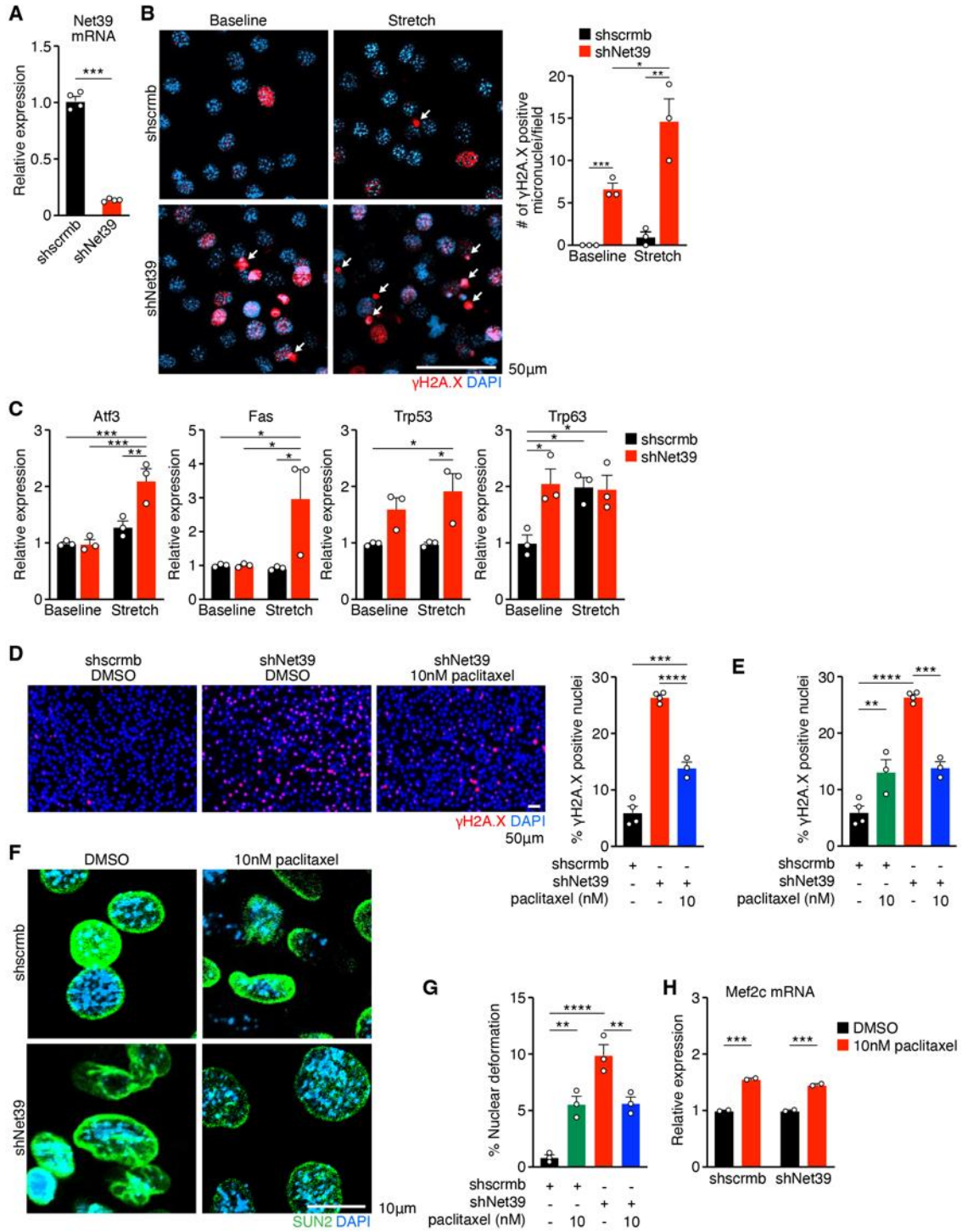


Supplemental Figure 2

Supplemental Figure 2 –cKO muscle displays myopathic features.

- a) Whole hindlimb immunostaining for type I (MYH7), type IIa (MYH2) and type IIb (MYH4) myofibers of Ctrl and cKO mice at 5 months of age. The magnified area (right) shows the presence of small angular fibers positive for MYH7 in cKO GP. Sections are co-stained with Laminin. Scale bar: middle 500 μ m, right 50 μ m.
- b) Immunostaining for type I (MYH7) and embryonic (MYH3) myosins (left), Desmin (middle), and cleaved caspase-3 (CL-CASP3) with WGA (right) in Ctrl and cKO GP muscle at 5 months of age. Scale bar: 50 μ m.
- c) Electron micrographs showing disorganized sarcomeres in cKO but not Ctrl GP muscle at 5 months of age. The small angular fiber with disorganized sarcomeres is outlined in the red borders. Scale bar: 4 μ m
- d) Hematoxylin and eosin staining (H&E) of GP muscles from Ctrl and cKO mice at 5 months and 9 months of age. Arrowheads indicate centralized nuclei. Scale bar: 50 μ m (left). Quantification of centralized nuclei from the same muscles (right). One-way ANOVA followed by Tukey's multiple comparisons test was performed to determine statistical significance. *** $p < 0.001$. N=3 mice per group and 50-100 nuclei were analyzed per mouse. Data represent mean \pm SEM.
- e) Masson's Trichrome staining of GP muscles from Ctrl and cKO mice at 5 months of age. Scale bar: 50 μ m (left). Quantification of fibrotic area from the same muscles (right). ** $p < 0.01$. Statistical comparisons between groups were evaluated by unpaired, two-tailed Student's t-test. N=3 mice per group. Data represent mean \pm SEM.

- f) Immunohistochemistry for CD11b from Ctrl and cKO muscles at 5 months of age
Scale bar: 50 μ m.
- g) Serum creatine kinase levels in Units (U) per liter (L) from Ctrl and cKO mice at 5 months of age. N=3 mice per group. Data represent mean \pm SEM.
- h) Protein levels of ATM, p-ATM, and γ H2A.X normalized to Vinculin (VCL) loading controls in the GP muscles from Ctrl and cKO mice at 5 months of age as detected by western blot analysis.
- i) Densitometry analysis of western blots for ATM, p-ATM and γ H2A.X protein levels from GP muscles from Ctrl and cKO mice at 5 months of age. * $p < 0.05$. Statistical comparisons between groups were evaluated by unpaired, two-tailed Student's t-test. N=2 mice per group. Data represent mean \pm SEM.



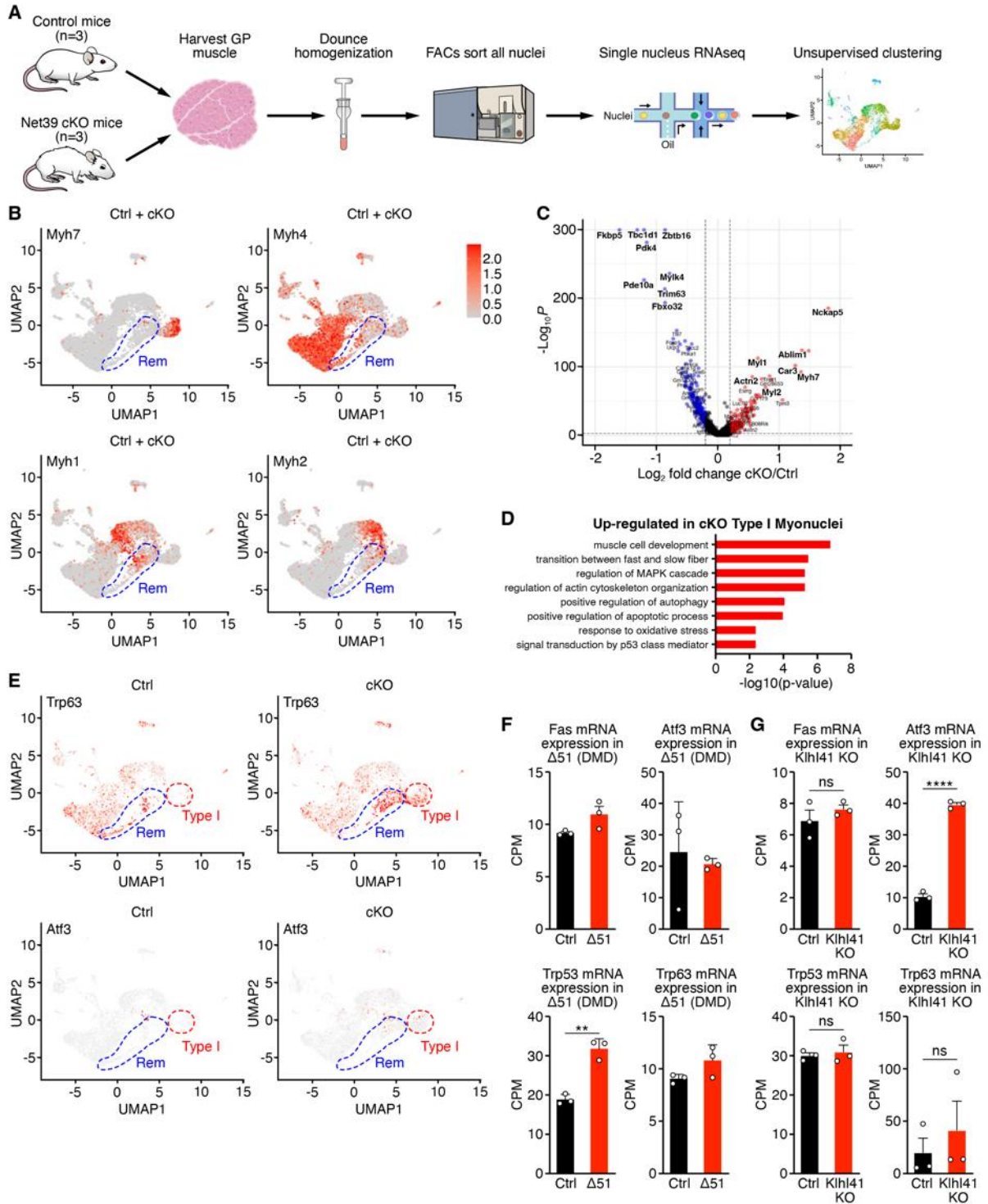
Supplemental Figure 3

Supplemental Figure 3 – Net39 knockdown in C2C12 myoblasts induce DNA damage, which is rescued by paclitaxel treatment.

- a) mRNA expression of *Net39* in C2C12 myotubes expressing scrambled shRNA (shscrm), or a shRNA targeting *Net39* (shNet39). N=3 independent experiments.
- b) Immunostaining for γ H2A.X (red) and DAPI showed γ H2A.X -positive micronuclei in shNet39 C2C12 myoblasts at baseline and after 1 hour of stretching (left). Quantification of the number of γ H2A.X-positive micronuclei per field (right). White arrows indicate γ H2A.X-positive micronuclei. * $p < 0.05$. ** $p < 0.01$. *** $p < 0.001$. Scale bar: 50 μ m. Statistical comparisons between groups were evaluated by unpaired, two-tailed Student's t-test. N=3 independent experiments and ~100 cells per experiment. Data represent mean \pm SEM.
- c) mRNA expression of DNA damage-induced genes in shscrm and shNet39 myoblasts at baseline and after 1 hour of stretching. Data were normalized to shscrm cells at baseline. * $p < 0.05$. ** $p < 0.01$, *** $p < 0.001$. Statistical comparisons between groups were evaluated by unpaired, two-tailed Student's t-test. N=3 independent experiments. Data represent mean \pm SEM.
- d) Immunostaining of γ H2A.X (red) and DAPI (blue) in shscrm and shNet39 C2C12 myoblasts following treatment with DMSO or 10nM paclitaxel. Scale bar: 50 μ m.
- e) Quantification of percentage of γ H2A.X-positive nuclei in shscrm and shNet39 C2C12 myoblasts following treatment with DMSO or 10nM paclitaxel. One-way ANOVA followed by Tukey's multiple comparisons test was performed to determine statistical significance. ** $p < 0.01$. *** $p < 0.001$. **** $p < 0.0001$. N=3-

4 independent experiments and ~100-500 cells per experiment. Data represent mean \pm SEM.

- f) Immunostaining of SUN2 (green) and DAPI (blue) in shscrmB and shNet39 C2C12 myoblasts following treatment with DMSO or 10nM paclitaxel. Scale bar: 10 μ m.
- g) Quantification of percentage of deformed nuclei in shscrmB and shNet39 C2C12 myoblasts following treatment with DMSO or 10nM paclitaxel. Deformed nuclei were identified using SUN2 staining. One-way ANOVA followed by Tukey's multiple comparisons test was performed to determine statistical significance. ** $p < 0.01$. **** $p < 0.0001$. N=3 independent experiments and ~100-500 cells per experiment. Data represent mean \pm SEM.
- h) mRNA expression of Mef2c in shscrmB and shNet39 following treatment with DMSO or 10nM paclitaxel. Data were normalized to shscrmB cells treated with DMSO. *** $p < 0.001$. Statistical comparisons between groups were evaluated by unpaired, two-tailed Student's t-test. N=2 independent experiments. Data represent mean \pm SEM.

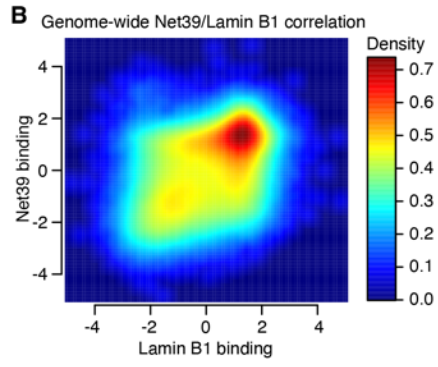
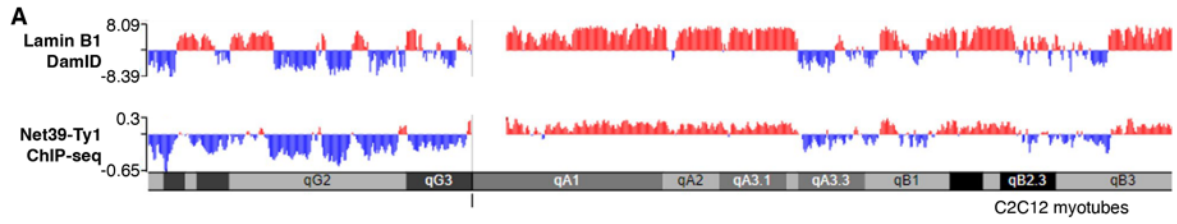


Supplemental Figure 4

Supplemental Figure 4 – Single nucleus RNA-seq identifies that pathological myonuclei express higher levels of DNA damage-induced genes.

- a) Schematic of the experimental design for snRNA-seq on skeletal muscle nuclei from Ctrl and cKO mice at 5 months of age.
- b) UMAP visualization of combined Ctrl and cKO expressions of different myosin isoforms from snRNA-seq data. Remodeling myonuclei show expression of *Myh7*, *Myh1*, *Myh2*, and *Myh4*. Remodeling myonuclei are enclosed in blue.
- c) Volcano plot illustrating the up- and down-regulated genes in Ctrl and cKO GP myonuclei (Type I, IIa, IIb, IIx, Rem) at 5 months of age by snRNA-seq.
- d) Gene Ontology (GO) Pathway analysis of the upregulated genes in cKO Type I myonuclei at 5 months of age by snRNA-seq.
- e) UMAP visualization of the expression of the DNA damage-related genes *Trp63* and *Atf3* in Ctrl and cKO, which showed an enrichment in cKO remodeling and type I myonuclei. Remodeling myonuclei are enclosed in blue. Type I myonuclei are enclosed in red.
- f) Transcript abundance measured by bulk RNA-seq of DNA damage-related genes in a mouse model of Duchenne muscular dystrophy (*Dmd* Δ Ex51) at 4 weeks of age. CPM: counts per million. ** $p < 0.01$. Statistical comparisons between groups were evaluated by unpaired, two-tailed Student's t-test. N=3 mice per group. Data represent mean \pm SEM.
- g) Transcript abundance measured by bulk RNA-seq of DNA damage-related genes in a mouse model of nemaline myopathy (*Kihl41* KO) at P0. CPM: counts per million. **** $p < 0.0001$. Statistical comparisons between groups were evaluated

by unpaired, two-tailed Student's t-test. N=3 mice per group. Data represent mean \pm SEM.



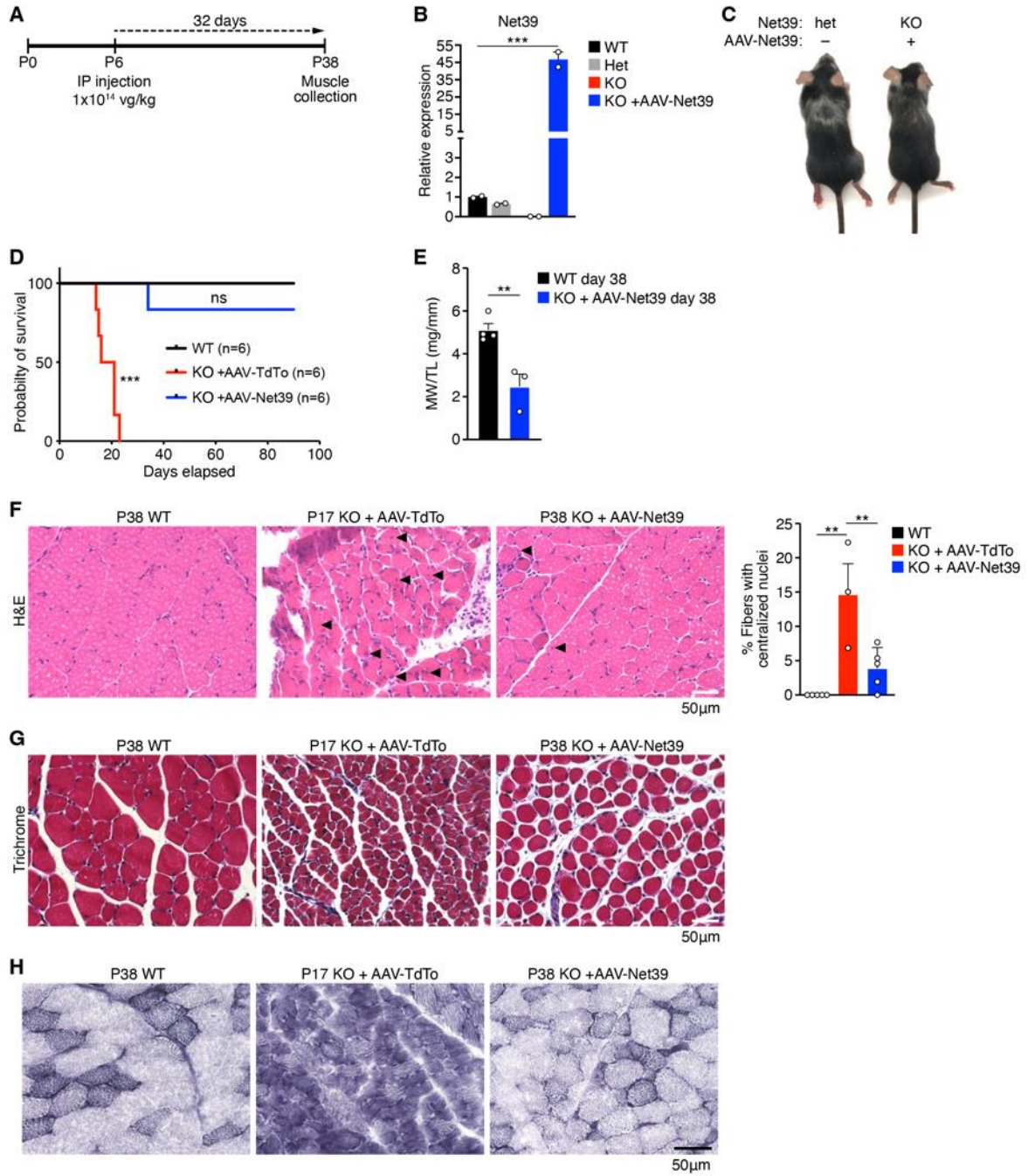
Supplemental Figure 5

Supplemental Figure 5 – Net39 binds DNA regions that resemble Lamin-associated domains

- a) LaminB1 DamID and Net39-Ty1 ChIPseq tracks shown for chromosome 6. Red indicates called Lamin B1 and Net39-Ty1 peaks. Chromosome arms are shown at the bottom.
- b) Correlation of Lamin B1 and Net39-Ty1 peaks for all chromosomes. X- and Y-axis values represent log ratios of ChIP signal to control for Net39-Ty1 and Lamin B1, respectively.

Supplemental Figure 6 – Mef2c is induced in cKO myonuclei along with its target genes.

- a) Violin plots showing the expression of Mef2c in all myonuclei (Type I, IIa, IIb, IIx, Rem) (left) and Type I myonuclei (right). P-values for expression comparison between Ctrl and cKO are shown. Statistical comparisons between groups were evaluated by unpaired, two-tailed Student's t-test.
- b) UMAP visualization of Ctrl and cKO expression of Mef2 family members Mef2a, Mef2c, and Mef2d expression. Type I myonuclei are enclosed in red.
- c) Dot-plots from snRNA-seq showing the expression of Mef2c target genes differentially expressed in Ctrl vs. cKO myonuclei. Red dots indicate upregulated genes and blue dots indicate downregulated genes in cKO.
- d) Mef2c mRNA expression in a mouse model of Duchenne muscular dystrophy (*Dmd* Δ Ex51). CPM: counts per million. ns: Not significant. N=3 mice.
- e) Mef2c mRNA expression in a mouse model of nemaline myopathy (*Kihl41* KO). CPM: counts per million. ns: Not significant. N=3 mice.
- f) Mef2c mRNA expression in shscrmB C2C12 myoblasts at baseline and after 1 hour of stretch. **p < 0.01. Statistical comparisons between groups were evaluated by unpaired, two-tailed Student's t-test. N=4 independent experiments.



Supplemental Figure 7

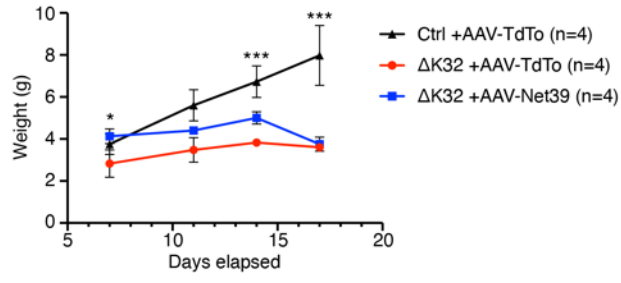
Supplemental Figure 7 – AAV-Net39 injection rescues the early lethality of *Net39* KO mice.

- a) Experimental design for the delivery of AAV-Net39 into Net39 global knockout (KO) mice. 1×10^{14} viral genomes (vg)/kilogram mouse weight (kg) of AAV were injected intraperitoneally (IP) at P6 and muscles were collected at P38.
- b) Net39 mRNA expression in GP muscles from Net39 KO mice at P38 injected with AAV-Net39 compared with wildtype (WT), heterozygote (Het), and KO mice. One-way ANOVA followed by Tukey's multiple comparisons test was performed to determine statistical significance. *** $p < 0.001$. N=2 mice per group. Data represent mean \pm SEM.
- c) Images of Het and KO mice uninjected (-) and injected (+) with AAV-Net39 at P38.
- d) Survival curves of WT (black) and KO mice injected with AAV-TdTo (red) or AAV-Net39 (blue). Log-rank (Mantel-Cox) test was performed to determine statistical significance. *** $p < 0.001$. N=6 mice per group.
- e) Quantification of muscle weight to tibia length ratios for WT (black) and KO mice injected with AAV-Net39 (blue) at P38. Statistical comparisons between groups were evaluated by unpaired, two-tailed Student's t-test. ** $p < 0.01$. N=3-4 mice per group. Data represent mean \pm SEM.
- f) Hematoxylin and eosin staining (H&E) of GP muscles from WT and KO mice injected with AAV-TdTo or AAV-Net39. KO + AAV-TdTo mice were analyzed at P17 whereas WT and KO + AAV-Net39 mice were analyzed at P38. Arrowheads indicate centralized nuclei. Scale bar: 50 μ m. Quantification of centralized nuclei

from the same muscles (right). ** $p < 0.01$. Statistical comparisons between groups were evaluated by unpaired, two-tailed Student's t-test. N=3-6 mice per group.

g) Masson's Trichrome staining of GP muscles from WT and KO mice injected with AAV-TdTo or AAV-Net39. KO + AAV-TdTo mice were analyzed at P17 whereas WT and KO + AAV-Net39 mice were analyzed at P38. Scale bar: 50 μ m.

h) NADH staining of GP muscles from WT and KO mice injected with AAV-TdTo or AAV-Net39. KO + AAV-TdTo mice were analyzed at P17 whereas WT and KO + AAV-Net39 mice were analyzed at P38. Scale bar: 50 μ m.



Supplemental Figure 8

Supplemental Figure 8 – AAV-Net39 injection modestly improves Δ K32 body weight.

Growth curves showing the body weight of Ctrl (black) and Δ K32 mice injected with AAV-TdTo (red) or AAV-Net39 (blue). One-way ANOVA followed by Tukey's multiple comparisons test was performed to determine statistical significance. ***
 $p < 0.001$ between Ctrl +AAV-TdTo mice and Δ K32 mice at P14 and P17. N=4 mice per group.